Supporting Information: Analytical Methods

Sample Selection & Petrography

Thirty-one representative polished thin sections from each mineralized vein stage and associated phyllically altered wallrock were selected for study from a comprehensive sample suite (n = 236 samples) collected during the lead author's PhD research on the Brucejack deposit (56° 27.994' N, 130° 11.215' W). The polished thin sections were chosen based on petrographic evidence for pyrite growth zoning as observed in reflected light (e.g., euhedral, inclusion-free grain rims surrounding corroded, inclusion-bearing cores). Four polished thin sections from each mineralized vein stage and associated wallrock were used for in situ trace element and sulfur isotope analyses (by electron microprobe and secondary ion mass spectrometry, respectively; see below) based on growth zoning confirmed by back-scattered electron (BSE) imaging.

Electron Microprobe Wavelength-Dispersive X-ray Spectroscopy (EMP-WDS)

The EMP-WDS analyses of pyrite were performed at the joint University of Ottawa–Canadian Museum of Nature MicroAnalysis Laboratory using a JEOL 8230 SuperProbe with five X-ray wavelength-dispersive spectrometers. Pyrite grains were quantitatively analyzed using the following X-ray lines: As (Lα), Au (Lα), Cu (Kα), Fe (Kα), and S (Kα). A combination of synthetic and natural standards, including Au80Ag20 alloy (Au), cubanite (Cu), GaAs alloy (As) and pyrite (Fe and S), were used for calibration. Microbeam analyses were performed using a beam energy of 20 kV, a 40° takeoff angle, a 2 µm beam diameter and a 200 nA beam current. Counting times for each element were set as follows: As (30 s), Au (200 s), Cu (30 s), Fe (10 s), and S (10 s). Detection limits (2σ) of 100 ppm As, 90 ppm Au, 80 ppm Cu, and 110 ppm Fe, and 70 ppm S were achieved using these operating conditions.

Secondary ion mass spectrometry (SIMS)

SIMS mount preparation and analysis were conducted at the Canadian Centre for Isotopic Microanalysis (CCIM), University of Alberta. Regions of interest 1.5 – 2.5 mm diameter were cored from polished thin-sections, and then cast into two 25 mm epoxy mounts (M1496, M1548) along with previously polished fragments of the primary CCIM pyrite reference material (S0302A). The mounts were lightly polished to a 0.25-micron finish using diamond pads, cleaned, and then coated

with 20 nm of Au prior to scanning electron microscopy (SEM). SEM characterization was carried out with a Zeiss EVO MA15 instrument using beam conditions of 20 kV and 3 – 5 nA. A further 80 nm of Au was subsequently deposited on the mounts prior to SIMS analysis.

Sulphur isotope ratios ($^{34}S/^{32}S$) were determined in pyrite using a IMS-1280 multi-collector ion microprobe. Primary beam conditions included the use of 20 keV $^{133}Cs^+$ ions focused to form a probe with diameters of 7 – 10 µm depending on requirements, with beam currents of ~0.2 – 0.6 nA. The primary beam, temporarily increased in intensity, was rastered across a 15 x 15 µm area for 30 s prior to analysis to implant Cs. The normal incidence electron gun was not utilized. Negative secondary ions were extracted through 10 kV potential to the grounded secondary column (Transfer section). Conditions for the Transfer section included an entrance slit width of 80 µm, field aperture of 5 x 5 mm, and a field aperture-to-sample magnification of 100x. Automated tuning of the secondary ions in the Transfer section preceded each analysis. The energy slit was fully open, and both secondary ion species were analyzed simultaneously using Faraday cups for $^{32}S^-$ and $^{34}S^-$ ($^{32}S^-$ in L'2 using $10^{11}\Omega$ amplifier circuits, $^{34}S^-$ in FC2 with $10^{11}\,\Omega$). Exit slit widths of 500 µm and ~270 µm were utilized for $^{32}S^-$ and $^{34}S^-$, respectively, that gave nominal mass resolutions of 2000 for $^{32}S^-$ (10% peak height definition) and 3500 for $^{34}S^-$. Faraday cup baselines were measured at the start of the session. Total between-spot analysis time was 200 s.

The analytical protocol involved interspersing analyses of pyrite reference material S0302A ($\delta^{34}S_{VCDT}$ = 0.0 ±0.2 ‰[1]) in a 4:1 or 5:1 ratio with unknowns. Pyrite S0302A is homogeneous at the micro-scale. The reference VCDT value utilized for $^{34}S/^{32}S = 0.0441626$[2]. Instrumental mass fractionation for $^{34}S^-/^{32}S^-$ was determined for the analytical sessions (IP18020A, IP18020B, IP19028) utilizing replicate analyses of S0302A pyrite. The standard deviations of $^{34}S^-/^{32}S^-$ ratios for S0302A were 0.05 – 0.08 ‰ for the sessions, after corrections for time-related IMF drift. Final uncertainties are reported at 95% confidence level (2σ) and propagate within-spot counting errors, between-spot errors to account for spatial and time-correlated (drift) uncertainties (±0.10 ‰ blanket error), and between-session errors that account for uncertainty in the mean IMF for the session. The total individual spot uncertainties in $\delta^{34}S_{VCDT}$ are typically ±0.2 ‰ (2σ).

References Cited

1. Liseroudi, M. H., Ardakani, O.H., Pedersen, P.K., Stern, R.A., Wood, J.M., and Sanei, H., Microbial and thermochemical controlled sulfur cycle in the Early Triassic sediments of the Western Canadian Sedimentary Basin. *Journal of the Geological Society* **178**, doi:10.1144/jgs2020-175 (2021).

2. Ding, T., Valkiers, S., Kipphardt, H., De Bièvre, P., Taylor, P. D. P., Gonfiantini, R., and Krouse, R., Calibrated sulfur isotope abundance ratios of three IAEA sulfur isotope reference materials and V-CDT with a reassessment of the atomic weight of sulfur. *Geochimica et Cosmochimica Acta* **65**, 2433–2437 (2001).

Supporting Information: Analytical Results

Table S1: EMP-WDS Results – Figure 2

Analysis ID	S WT%	Fe WT%	Cu WT%	Au WT%	As WT%	TOTAL
U_1380x24V3a_pyrite_spot_1	49.98	45.10	-	0.013	4.59	99.76
U_1380x24V3a_pyrite_spot_2	53.75	46.66	-	-	-	100.40
U_1380x24V3a_pyrite_spot_3	53.92	46.14	-	-	-	100.10
U_1380x24V3a_pyrite_spot_4	52.26	44.23	0.16	0.010	2.79	99.45
U_1380x24V3a_pyrite_spot_5	52.41	44.36	0.21	0.015	2.75	99.74

Table S2: EMP-WDS Results – Figure 3

Analysis ID	S WT%	Fe WT%	Cu WT%	Au WT%	As WT%	TOTAL
SU-021-361a_pyrite_spot_1	52.00	44.94	-	-	1.37	98.32
SU-021-361a_pyrite_spot_2	52.15	45.26	-	-	1.07	98.48
SU-021-361a_pyrite_spot_3	51.36	44.65	-	-	2.42	98.45
SU-021-361a_pyrite_spot_4	52.19	45.33	-	-	1.27	98.80
SU-021-361a_pyrite_spot_5	52.46	44.99	-	-	1.19	98.65
SU-021-361a_pyrite_spot_6	52.33	45.33	-	-	1.22	98.89
SU-021-361a_pyrite_spot_7	53.16	45.36	-	-	0.26	98.79
SU-021-361a_pyrite_spot_8	52.10	45.07	-	-	1.21	98.39

Table S3: SIMS Results – Figure 2 – Transect A-A'

Spot Name	$^{34}S/^{32}S$	$\delta^{34}S$ (VCDT)	2σ (‰) inter-session
S5103B_A-A'@1	0.0441855	0.52	0.16
S5103B_A-A'@2	0.0441485	-0.32	0.15
S5103B_A-A'@3	0.0441113	-1.16	0.15
S5103B_A-A'@4	0.0441116	-1.15	0.14
S5103B_A-A'@5	0.0440986	-1.45	0.17
S5103B_A-A'@6	0.0438565	-6.93	0.14
S5103B_A-A'@7	0.0434223	-16.76	0.21
S5103B_A-A'@8	0.0441073	-1.25	0.14

Table S4: SIMS Results – Figure 2 – Transect B-B'

Spot Name	$^{34}S/^{32}S$	$\delta^{34}S$ (VCDT)	2σ (‰) inter-session
S5103B_B-B'@1	0.0441560	-0.15	0.15
S5103B_B-B'@2	0.0442170	1.23	0.14
S5103B_B-B'@3	0.0441095	-1.20	0.18
S5103B_B-B'@4	0.0441265	-0.82	0.15
S5103B_B-B'@5	0.0441136	-1.11	0.15
S5103B_B-B'@6	0.0436596	-11.39	0.25
S5103B_B-B'@7	0.0438165	-7.84	0.22
S5103B_B-B'@8	0.0438169	-7.83	0.20
S5103B_B-B'@9	0.0435572	-13.71	0.23
S5103B_B-B'@10	0.0437781	-8.71	0.17
S5103B_B-B'@11	0.0435313	-14.29	0.15
S5103B_B-B'@12	0.0434399	-16.36	0.15
S5103B_B-B'@13	0.0434026	-17.21	0.14
S5103B_B-B'@14	0.0435450	-13.98	0.12
S5103B_B-B'@15	0.0435844	-13.09	0.17
S5103B_B-B'@16	0.0435511	-13.85	0.15
S5103B_B-B'@17	0.0434018	-17.23	0.21
S5103B_B-B'@18	0.0437343	-9.70	0.20
S5103B_B-B'@19	0.0433322	-18.80	0.14
S5103B_B-B'@20	0.0429983	-26.36	0.19
S5103B_B-B'@21	0.0430584	-25.00	0.13
S5103B_B-B'@22	0.0441397	-0.52	0.14
S5103B_B-B'@23	0.0444294	6.04	0.17

Table S5: SIMS Results – Figure 2 – Transect C-C'

Spot Name	$^{34}S/^{32}S$	$\delta^{34}S$ (VCDT)	2σ (‰) inter-session
S5103B_C-C'@1	0.0431843	-22.15	0.26
S5103B_C-C'@2	0.0439647	-4.48	0.20
S5103B_C-C'@3	0.0433113	-19.28	0.17
S5103B_C-C'@4	0.0433297	-18.86	0.18
S5103B_C-C'@5	0.0435802	-13.19	0.15
S5103B_C-C'@6	0.0433552	-18.28	0.18
S5103B_C-C'@7	0.0441372	-0.57	0.12
S5103B_C-C'@8	0.0445151	7.98	0.15

Table S6: SIMS Results – Figure 2 – Eastern Spots

Spot Name	$^{34}S/^{32}S$	$\delta^{34}S$ (VCDT)	2σ (‰) inter-session
S5103B_XSE@1	0.0441837	0.48	0.16
S5103B_XSE@2	0.0442145	1.18	0.16
S5103B_XSE@3	0.0441731	0.24	0.17
S5103B_XSE@4	0.0441739	0.26	0.19
S5103B_XSE@5	0.0441807	0.41	0.13
S5103B_XSE@6	0.0441918	0.66	0.16
S5103B_XSE@7	0.0441337	-0.65	0.15
S5103B_XSE@8	0.0441387	-0.54	0.13
S5103B_XSE@9	0.0441829	0.46	0.17
S5103B_XSE@10	0.0441947	0.73	0.14
S5103B_XSE@11	0.0441320	-0.69	0.17
S5103B_XSE@12	0.0441286	-0.77	0.13
S5103B_XSE@13	0.0441290	-0.76	0.13
S5103B_XSE@14	0.0441517	-0.25	0.15
S5103B_XSE@15	0.0441890	0.60	0.14
S5103B_XSE@16	0.0441837	0.48	0.17
S5103B_XSE@17	0.0441444	-0.41	0.17
S5103B_XSE@18	0.0441376	-0.57	0.13
S5103B_XSE@19	0.0436514	-11.57	0.18
S5103B_XSE@20	0.0441402	-0.51	0.14
S5103B_XSE@21	0.0436467	-11.68	0.24
S5103B_XSE@22	0.0441606	-0.05	0.15

Table S7: SIMS Results – Figure 3a – Transect D-D'

Spot Name	$^{34}S/^{32}S$	$\delta^{34}S$ (VCDT)	2σ (‰) inter-session
S5106B_D-D'@1	0.0441647	0.05	0.18
S5106B_D-D'@2	0.0441931	0.69	0.15
S5106B_D-D'@3	0.0075600	-1.28	0.15
S5106B_D-D'@4	0.0441223	-0.91	0.17
S5106B_D-D'@5	0.0442210	1.32	0.18
S5106B_D-D'@6	0.0442135	1.15	0.15
S5106B_D-D'@7	0.0442302	1.53	0.17
S5106B_D-D'@8	0.0442867	2.81	0.25
S5106B_D-D'@9	0.0443804	4.93	0.15
S5106B_D-D'@10	0.0444051	5.49	0.22
S5106B_D-D'@11	0.0444448	6.39	0.21
S5106B_D-D'@12	0.0444738	7.05	0.17
S5106B_D-D'@13	0.0444926	7.47	0.25
S5106B_D-D'@14	0.0445335	8.40	0.18
S5106B_D-D'@15	0.0445682	9.19	0.25
S5106B_D-D'@16	0.0446105	10.14	0.12
S5106B_D-D'@17	0.0446243	10.46	0.19
S5106B_D-D'@18	0.0446638	11.35	0.28
S5106B_D-D'@19	0.0447136	12.48	0.19
S5106B_D-D'@20	0.0447293	12.83	0.12
S5106B_D-D'@21	0.0447615	13.56	0.21
S5106B_D-D'@22	0.0449883	18.70	0.20
S5106B_D-D'@23	0.0450663	20.46	0.17
S5106B_D-D'@24	0.0451315	21.94	0.20
S5106B_D-D'@25	0.0451465	22.28	0.18
S5106B_D-D'@26	0.0452219	23.99	0.19

Table S8: SIMS Results – Figure 3a – Transect D-D' Peripheral Spots

Spot Name	$^{34}S/^{32}S$	$\delta^{34}S$ (VCDT)	2σ (‰) inter-session
S5106B_D-D'_PS@1	0.0451163	21.60	0.19
S5106B_D-D'_PS@2	0.0446709	11.51	0.16
S5106B_D-D'_PS@3	0.0443768	4.85	0.17
S5106B_D-D'_PS@4	0.0440718	-2.05	0.16

Table S9: SIMS Results – Figure 3a – Northern Spots

Spot Name	$^{34}S/^{32}S$	$\delta^{34}S$ (VCDT)	2σ (‰) inter-session
S5106B_XSN@1	0.0442035	0.93	0.13
S5106B_XSN@2	0.0443857	5.04	0.20
S5106B_XSN@3	0.0443866	5.07	0.22
S5106B_XSN@4	0.0444742	7.06	0.18
S5106B_XSN@5	0.0446946	12.05	0.19
S5106B_XSN@6	0.0447015	12.20	0.16
S5106B_XSN@7	0.0451225	21.74	0.21
S5106B_XSN@8	0.0441440	-0.42	0.17
S5106B_XSN@9	0.0439807	-4.12	0.16
S5106B_XSN@10	0.0441089	-1.22	0.18

Table S10: SIMS Results – Figure 3b – Transect E-E'

Spot Name	$^{34}S/^{32}S$	$\delta^{34}S$ (VCDT)	2σ (‰) inter-session
S5778B1_E-E'@1	0.0447336	8.32	0.14
S5778B1_E-E'@2	0.0442431	-2.79	0.15
S5778B1_E-E'@3	0.0442799	-1.96	0.12
S5778B1_E-E'@4	0.0443036	-1.43	0.14
S5778B1_E-E'@5	0.0443243	-0.96	0.17
S5778B1_E-E'@6	0.0447356	8.36	0.17
S5778B1_E-E'@7	0.0445475	8.72	0.17
S5778B1_E-E'@8	0.0444683	6.92	0.14
S5778B1_E-E'@9	0.0443283	3.75	0.15
S5778B1_E-E'@10	0.0437954	-8.31	0.13
S5778B1_E-E'@11	0.0428096	-30.64	0.12
S5778B1_E-E'@12	0.0425698	-36.06	0.19
S5778B1_E-E'@13	0.0433534	-18.32	0.15
S5778B1_E-E'@14	0.0438675	-6.68	0.22

Figure S1

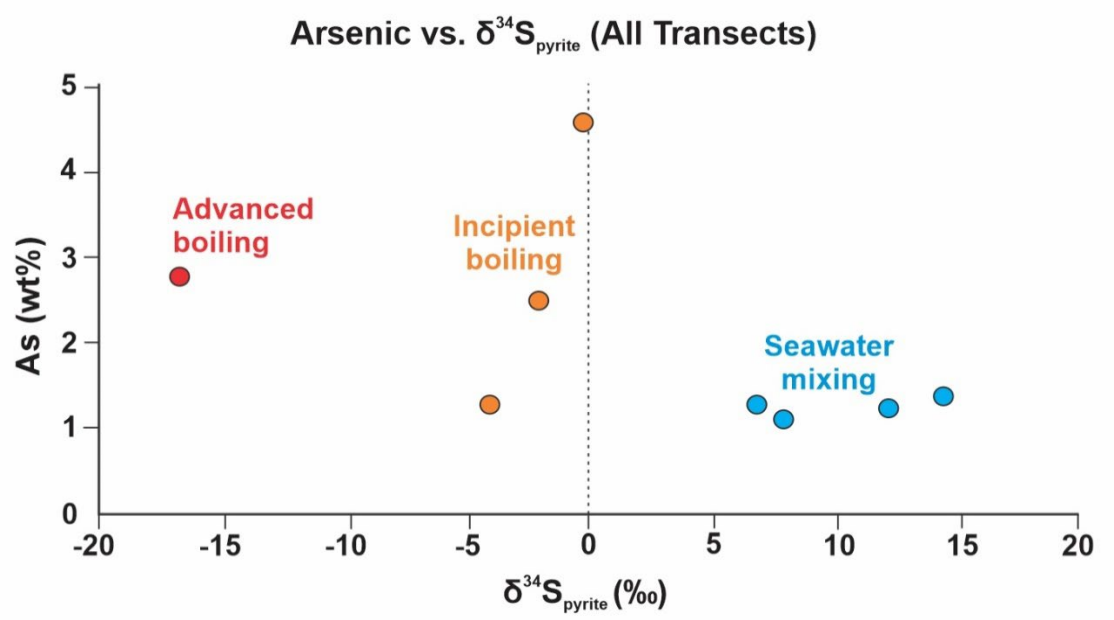

Figure S1: plot of arsenic concentration in pyrite vs. $\delta^{34}S_{pyrite}$ from the results of analyses illustrated in Figures 2 and 3 (results are only shown for analysis sites which have both EMPA As and SIMS $\delta^{34}S$ data available). The symbols in orange, red, and blue are interpreted to correspond to the onset of boiling, advanced boiling, and seawater mixing, respectively. See the main manuscript for further discussion.